EBioMedicine 42 (2019) 524–531

Contents lists available at ScienceDirect

EBioMedicine

journal homepage: www.ebiomedicine.com

EBioMedicine
Published by THE LANCET

A truncating MEIOB mutation responsible for familial primary ovarian insufficiency abolishes its interaction with its partner SPATA22 and their recruitment to DNA double-strand breaks

Sandrine Caburet [a,b,1], Anne-Laure Todeschini [a,b,1], Cynthia Petrillo [b,c,d], Emmanuelle Martini [b,c,d], Nada D. Farran [e], Bérangère Legois [a,b], Gabriel Livera [b,c,d], Johnny S. Younis [f,*], Stavit Shalev [e,g,2], Reiner A. Veitia [a,b,*,2]

[a] Institut Jacques Monod, Université Paris Diderot, CNRS UMR7592, Paris 75013, France
[b] Université Paris Diderot-Paris 7, 75205 Paris Cedex 13, France
[c] UMR1274, Genetic Stability Stem Cells and Radiation, CEA/DRF/iRCM/SCSR/LDG, Fontenay aux Roses F-92265, France
[d] Université Paris-Sud, Paris, Saclay, France
[e] OBGYN Department, Genetic Institute, Haemek Medical Center, Afula, Israel
[f] Baruch Padeh Medical Center, Poriya, The Azrieli Faculty of Medicine, Bar-Ilan University, Safed, Israel
[g] Genetic Institute, Emek Medical Center, Israel

ARTICLE INFO

Article history:
Received 28 February 2019
Received in revised form 20 March 2019
Accepted 26 March 2019
Available online 15 April 2019

Keywords:
Exon skipping
Female infertility
MEIOB
Meiotic recombination
Primary ovarian insufficiency

ABSTRACT

Background: Primary Ovarian Insufficiency (POI), a major cause of infertility, affects about 1–3% of women under forty years of age. Although there is a growing list of causal genetic alterations, POI remains mostly idiopathic.
Methods: We performed exome sequencing (WES) of two sisters affected with POI, one unaffected sister and their mother from a consanguineous family. We assessed the impact of the identified *MEIOB* variant with a minigene assay and by sequencing illegitimate transcripts from the proband's leukocytes. We studied its functional impact on the interaction between MEIOB with its partner SPATA22 and their localization to DNA double-strand breaks (DSB).
Findings: We identified a homozygous variant in the last base of exon 12 of *MEIOB*, which encodes a factor essential for meiotic recombination. This variant was predicted to strongly affect *MEIOB* pre-mRNA splicing. Consistently, a minigene assay showed that the variant induced exon 12 skipping, which was confirmed *in vivo* in the proband's leukocytes. Aberrant splicing leads to the production of a C-terminally truncated protein that cannot interact with SPATA22, abolishing their recruitment to DSBs.
Interpretation: This truncating MEIOB variant is expected to provoke meiotic defects and a depleted follicular stock, as in *Meiob*$^{-/-}$ mice. This is the first molecular defect reported in a meiosis-specific single-stranded DNA-binding protein (SSB) responsible for POI. We hypothesise that alterations in other SSB proteins could explain cases of syndromic or isolated ovarian insufficiency.
Fund: Université Paris Diderot, Fondation pour la Recherche Médicale, Fondation ARC contre le cancer, Commissariat à l'Energie Atomique and Institut Universitaire de France.

1. Introduction

Primary ovarian insufficiency (POI) affects about 1–3% of women under 40 years of age. POI patients have amenorrhea for at least 6 months and high FSH levels. POI stems from a depletion of the ovarian follicle pool and can be observed isolated or in syndromic conditions. About 10–15% of POI cases have a genetic etiology but most cases remain idiopathic [1,2]. However, an increasing number of genetic alterations have been described in women with POI [3]. In particular, pathogenic variants in genes involved in DNA replication, recombination or repair, such as *STAG3*, *SYCE1*, *MCM8*, *MCM9*, and *HFM1*, have been formally implicated in this condition [4–8].

Here, we have applied exome sequencing (WES) to a consanguineous family of Arab origin with two sisters affected with POI. This analysis allowed us to identify a damaging homozygous variant in the last base

* Corresponding authors at: J. S Younis, Baruch Padeh Medical Center, Poriya, The Azrieli Faculty of Medicine, Bar-Ilan University, Safed, Israel; R.A. Veitia, Institut Jacques Monod, Université Paris Diderot, CNRS UMR7592, Paris 75013, France
E-mail addresses: jsy@netvision.net.il (J.S. Younis), reiner.veitia@ijm.fr (R.A. Veitia).
[1] Equally contributing authors.
[2] co-last authors

https://doi.org/10.1016/j.ebiom.2019.03.075

Research in context

Evidence before the study

Primary Ovarian Insufficiency (POI), also called premature menopause, is a condition that affects about 1–3% of women under forty years of age. It is accompanied by infertility, hormonal changes and steroid-deprivation symptoms such as osteoporosis and neurodegenerative diseases. The causes of this condition are unknown in most cases but genetic factors appear to play an important role. Indeed, there is a growing, yet incomplete, list of genetic alterations that lead to POI.

Added value of this study

To get insights into this disorder, we have sequenced the coding part of the genome of two sisters affected with POI, one unaffected sister and their unaffected mother, all belonging to a consanguineous family where the parents are double first cousins. As a result of our genomic exploration, we found a DNA alteration in the *MEIOB* gene, which leads to the production of a truncated protein in the two patients. This gene is basically expressed in the oocyte and is involved in the recombination of the genetic material. Our analyses show that the mutated protein is unable to play its normal role, potentially leading to DNA repair defects that end up causing POI. Our results are consistent with the infertility observed in female mice without *Meiob*.

Implications of all the available evidence

We have uncovered the first cases implicating *MEIOB* biallelic alterations in POI. Our findings further support a genetic link between female infertility and DNA recombination and increase the number of genes whose alterations are involved in POI. They will improve the diagnosis and counselling of patients with POI and their families.

of exon 12 of the *MEIOB* gene. *MEIOB* encodes a meiosis-specific factor involved in homologous recombination. This protein is conserved among metazoan species and contains single-stranded DNA (ssDNA) binding domains similar to those of RPA1 (Replication protein A1), the large subunit of the ubiquitous single-stranded DNA-binding (SSB) protein complex RPA [9,10]. MEIOB is involved in ssDNA binding during the repair of meiotic double strand breaks (DSB). It is required for proper meiotic recombination in complex with SPATA22 (spermatogenesis associated 22), and has been shown to interact with RPA [11,12]. Minigene assays and the analysis of illegitimate *MEIOB* transcripts in the proband's leukocytes showed that the pathogenic variant leads to exon 12 skipping, leading to the production of a truncated protein which cannot be recruited to DSBs. Our findings are consistent with the phenotype of the *Meiob*$^{-/-}$ mouse that displays infertility in both sexes due to meiotic arrest. This is the first report of a clearly pathogenic variant of an SSB protein leading to female infertility.

2. Materials and methods

2.1. Exome sequencing

This study was approved by the Ethical Committee of the Emek Medical Center (EMC-0044-16). Written informed consent was obtained from all individuals included in the study. Genomic DNA was extracted from fresh blood samples by standard methods. Library preparation, exome capture, sequencing, and data analysis were performed by IntegraGen SA (Evry, France). Sequence capture, enrichment, and elution were performed according to manufacturer's instructions and protocols (SureSelect Clinical Research Exome V2, Agilent Technologies) without modification except for library preparation performed with NEBNext® Ultra kit (New England Biolabs®). For library preparation, 600 ng of each genomic DNA was fragmented by sonication and purified to yield fragments of 150–200 bp. Paired-end adaptor oligonucleotides from the NEB kit were ligated onto the repaired fragments then purified and enriched with 8 PCR cycles. 1200 ng of purified libraries were then hybridised to the SureSelect oligo probe capture library for 72 h. After hybridization, washing, and elution, the eluted fraction was PCR-amplified (9 cycles), purified and quantified by qPCR to obtain sufficient template DNA for downstream applications. Each eluted-enriched DNA sample was then sequenced on an Illumina HiSeq4000 as Paired End 75 bases reads. Image analysis and base calling was performed using Illumina Real Time Analysis (2.7.7) with default parameters. For detailed explanations of the process, see Gnirke et al. [13].

2.2. Bioinformatics

Base-calling was performed by using the Real-Time Analysis software sequence pipeline (2.7.7) with default parameters. Sequence reads were mapped onto the human genome build (hg38/GRCh38) by using the Burrows-Wheeler Aligner (BWA) tool. Duplicated reads (*e.g.* paired-end reads in which the insert DNA molecule showed identical start and end locations in the human genome) were removed using sambamba tools. The Whole Exome Sequencing metrics are provided in Table S1.

Variant calling, allowing the identification of SNV (Single Nucleotide Variations) and small insertions/deletions (up to 20 bp) was performed *via* the Broad Institute GATK Haplotype Caller GVCF tool (3.7) for constitutional DNA. Ensembl's VEP (Variant Effect Predictor, release 87) program was used for initial variant annotation. This tool takes into account data available in dbSNP (dbSNP147), the 1000 Genomes Project (1000G_phase3), the Exome Variant Server (ESP6500SI-V2-SSA137), the Exome Aggregation Consortium (ExAC r3.0), and IntegraGen in-house databases. For missense changes, two bioinformatic predictions for pathogenicity are available: SIFT (SIFT.2.2), PolyPhen (2.2.2). Other information like quality score, homozygote/heterozygote status, count of variant allele reads, presence of the variant in the COSMIC database (version79) are reported. Additional annotation data was retrieved using dbNSFP (version 3.4, https://sites.google.com/site/jpopgen/dbNSFP) and Varsome (https://varsome.com/). Minor allele frequencies were manually verified on GnomAD (http://gnomad.broadinstitute.org), ISB Kaviar (http://db.systemsbiology.net/kaviar/), and Great Middle Eastern variant database GME Variome: (http://igm.ucsd.edu/gme/).

Variant filtering was performed on the following criteria:

- minimum depth at variant position of 5,
- correct segregation in the family, on the basis of homozygosity by descent: variants should be homozygous in both affected sisters III-10 and III-11, heterozygous in the mother II-8 (obligate carrier), heterozygous or homozygous for Reference allele in the fertile sister III-13,
- absence in unrelated in-house fertile controls,
- Minor Allele Frequency (MAF) below 1% both in global and in each population in the GnomAD database,
- presence in the coding sequence (i.e not in UTRs, introns, intergenic, …)
- high predicted functional impact on the protein. Impact was evaluated based on the nine predictors included in dbNSFP [14–16] plus M-CAP [17] (considered as pathogenic when the majority of the predictors agreed). For splicing-altering variants, we kept the variants with a predicted impact on splicing using ADA Score and Random Forest (RF) probabilities above 0.6 [18]. The numbers of variants

fulfilling those criteria are given in Table S2. Visual inspection of the variant was performed using the IGV viewer (see Fig. S1a).

2.3. Variant confirmation by Sanger sequencing

The genomic region including the variant c.1218G>A was PCR-amplified (see Table S3 for all primers used in this study), sequenced with the Big Dye Terminator Kit (Applied Biosystems), and analysed using the ABI PRISM 3100 Genetic Analyzer (Applied Biosystems) according to the manufacturer's instructions. The chromatograms are displayed in Fig. S1b.

2.4. In vitro analysis of exon skipping

2.4.1. miniMEIOB expression constructs

The plasmids driving the expression of wild-type *MEIOB* minigene (miniMEIOB) were constructed by fusion PCR. Briefly, four PCRs were performed to generate each exon (from Exon 11 to 14) surrounded by 200pb of intron sequence (as the full intron sequences could not be amplified). PCRs were performed using DNA from the genomic Clone IMGSB737G051023D (CTD-2522J7, Source BioScience) as a template. After purification, the PCR products were mixed in equimolar amounts and allowed to undergo ten cycles of PCR in the absence of primers, to generate the full-length miniMEIOB. Then, a final PCR reaction was performed using the forward and reverse MEIOB primers (see Table S3 for primers, purchased from Sigma-Aldrich (St Louis, MO)). The amplified miniMEIOB was cloned in a pcDNA3.1 TOPO-TA vector from Invitrogen. The variant 1218G>A was then introduced in miniMEIOB WT gene by fusion PCR. First, two PCR reactions were performed to generate the 5′ and 3′ fragments of the mutated miniMEIOB gene using MEIOBForward primer and the corresponding mutagenic R primer MEIOB-Fusion-R and mutagenic MEIOB-Fusion-F primer along with MEIOBReverse (subsequent steps: as described above). All constructs were verified by Sanger sequencing to exclude the presence of PCR-induced mutations.

2.4.2. Cell culture and minigene assays

HeLa cells were used for minigene assays (CLS Cat# 300194/p772_HeLa, RRID:CVCL_0030). Cells were grown in DMEM-F12 medium (Gibco®, Life Technologies, Grand Island, NY, USA), supplemented with 10% fetal bovine serum (FBS) and 1% penicillin/streptomycin (Invitrogen-Gibco, Life Technologies, Grand Island, NY, USA). Cells were seeded 16 h before transfection to be at 80% of confluence at the time of transfection and transfected with 6250 ng of total DNA per well (6-well plates) using the calcium phosphate method [19] and rinsed 24 h after transfection. Forty-eight hours after transfection, cells were washed with phosphate-buffered saline before mRNA extraction with TRI Reagent® (MRC, Euromedex) according to the manufacturer's instructions. cDNA synthesis was performed using M-MLV (Invitrogen) and random hexamers. Altered splicing/exon skipping was assessed by RT-PCR on miniMEIOB mRNA with MEIOBForward and MEIOBReverse primers.

2.5. In vivo illegitimate MEIOB mRNA expression assays

2.5.1. RNA isolation and RT-PCR

Total RNA extractions from the proband and a fertile control fresh blood samples were performed using the TRI reagent (Sigma). For RT-PCR reactions, 1 μg of total RNA was amplified using the qScript cDNA Synthesis Kit (Quanta bio) in a final volume of 20 μl. The final mixture was incubated for 5 min at 22 °C, 30 min at 42 °C, and 5 min at 85 °C to inactivate the enzymes.

2.5.2. Expression analysis

Nested PCR was used to evaluate the expression profile of the wild-type and mutated transcripts. PCR were carried out with two nested pairs of primers to amplify the *MEIOB* cDNA between exons 11 and 14, expected to amplify 501 bp (external PCR, wild-type allele) and 386 bp (nested PCR, wild-type allele, see Table S3). Amplification was performed for 40 cycles, 94 °C for 30 s, 55 °C for 45 s and 72 °C for 1 min. PCR products were verified by Sanger sequencing. Longer fragments of the sequencing chromatograms are displayed in Fig. S2.

2.6. Biochemical assays

2.6.1. Cell culture and plasmid transfections

Cells were cultivated in a 5% CO_2 humidified incubator at 37 °C. Human embryonic kidney cells (HEK-293, ATCC, CLS Cat# 300192, RRID:CVCL_0045) and HeLa cells were grown in DMEM supplemented with 10% FBS (Gibco). Plasmid transfection was performed with Lipofectamine 2000 (Life Technologies) according to the manufacturer's instructions.

2.6.2. Plasmid constructs

All enzymes are from New England Biolabs (Ipswich, MA), antibiotics and primers from Sigma-Aldrich (St Louis, MO). Primer sequences are provided in Table S3. All PCR were performed using Phusion DNA polymerase. All constructs were Sanger-sequenced. To express 3xHA N-terminal-tagged full-length human SPATA22, the desired fragment of human SPATA22 cDNA from pCMV6-XL5- HsSPATA22 (Origene, cat# SC123038) was amplified by PCR and the PCR product digested by *Eco*RI and BamHI and cloned into a pKH3 plasmid (Addgene). Human MYC-FLAG tagged MEIOB was expressed using pCMV6-HsMEIOB-MYC-FLAG (Origene, cat# RC228391).

2.6.2.1. pCIG-MCS-IRES (SC0583 plasmid). pCIG plasmid containing MEIOB from pCMV6-HsMEIOB-MYC-FLAG (Origene, cat# RC228391) was modified to remove the EGFP coding sequence and to introduce multiple cloning site (MCS) sequences upstream and downstream of the IRES sequence. In order to add MCS sequences, the pCIG plasmid was amplified with primers SP0629 and SP0630. The resulting PCR product was used as a template for an additional amplification with SP0631 and SP0632 adding homology sequences to pCIG plasmid. After purification (GeneJet PCR – ThermoFisher Scientific, Waltham, MA), the PCR product was treated with T4 DNA polymerase for complementary single-strand annealing cloning with T4-DNA-polymerase-treated pCIG plasmid already digested by *Xho*I + *Bgl*II. The resulting plasmid was called pCIG-MCS-IRES (SC0583 plasmid).

2.6.2.2. pCIG-HsMEIOB-1-471-cMyc-Flag-IRES-HsSPATA22-1-363 (SC0585); expression vector for SPATA22 and the wild-type form of MEIOB. First, the HsSPATA22-1-363 coding sequence was amplified from pET15b-HsSPATA22-1-363 (obtained by subcloning HsSPATA22-1-363 from pCMV6-XL5- HsSPATA22 (Origene, cat# SC123038 with Nde1 and BamHI) with SP0636 and SP0637 primers. The resulting PCR product was digested by *Msc*I + BglII and ligated in the SC0583 plasmid digested by the same enzymes and treated with Fast-AP (Alkaline Phosphatase, ThermoFisher), thus generating pCIG-MCS-IRES-HsSPATA22-1-363 plasmid. Then, the HsMEIOB-1-471-cMyc-Flag coding sequence was amplified from pCMV6-HsMEIOB-1-471 (Origene, cat# RC228391) with SP0633 and SP0635. The resulting PCR product was digested by *Eco*RI-HF + *Xma*I and ligated in pCIG-MCS-IRES-HsSPATA22-1-363 digested by the same enzymes and treated with Fast-AP (ThermoFisher) generating pCIG-HsMEIOB-1-471-cMyc-Flag-IRES-HsSPATA22-1-363 (SC0585 plasmid).

2.6.2.3. pCIG-HsMEIOB-1-344-WYMSFLQ-cMyc-Flag-IRES-HsSPATA22-1-363 (SC0896); to express SPATA22 end the truncated form of MEIOB. The HsMEIOB-1-344-WYMSFLQ coding sequence was synthetised with additional homologous sequences to SC0585 and sub-cloned into a pUC57-like plasmid (Proteogenix, Schiltigheim, France). The sequence of interest was released by *Bbs*I digestion and cloned instead of the

HsMEIOB-1-471 wild-type sequence by complementary single-strand annealing cloning in SC0585 digested by *Eco*RI-HF and *Mlu*I-HF, thus generating SC0896.

2.6.3. Co-immunoprecipitation

HEK-293 cells were lysed under native conditions by homogenisation in 1× cell lysis buffer (Cell Signaling Technology, Leiden, The Netherlands) supplemented with complete protease inhibitor (Roche), PMSF, and 10 μM MG-132 (Sigma-Aldrich, St Louis, MO), 2 × 10 min of medium sonication (30 s on, 30 s off), and centrifugation at 16,200*g* for 10 min at 4 °C. Extracts were diluted 4× in binding buffer (20 mM Tris-HCl, pH 7.5, 150 mM NaCl, 10% glycerol, 1 mM EDTA, 1 mM beta-mercaptoethanol, 10 mg/ml BSA, complete protease inhibitor without EDTA (Roche), 10 μM MG-132, and 90 U/ml Benzonase nuclease (Novagen, Darmstadt, Germany), PMSF). Extracts from ~5 × 10^6 cells were used for IP with 25 μl of anti-FLAG M2 magnetic beads (Sigma-Aldrich, St Louis, MO, Cat# M8823, RRID:AB_2637089). The protein/beads mixture was incubated for 16 h at 4 °C with gentle agitation. To optimise Benzonase digestion after the binding reaction, the beads were washed twice with Benzonase buffer (20 mM Tris-HCl, pH 8.0, 20 mM NaCl, 10% glycerol, 2 mM $MgCl_2$, 1 mM beta-mercaptoethanol, 10 mg/ml BSA, complete protease inhibitor without EDTA, Roche) and incubated in Benzonase buffer supplemented with 90 U/ml Benzonase nuclease for 30 min at 37 °C before being washed three times with rinsing buffer (20 mM Tris-HCl, pH 7.5, 150 mM NaCl, 10% glycerol, 1 mM EDTA, 1 mM beta-mercaptoethanol, complete protease inhibitor without EDTA, triton 0.25%). Immunoprecipitated proteins were eluted directly in 18 μl of Laemmli buffer 1.5× supplemented with 0.5% beta-mercaptoethanol and boiled for 5 min at 95 °C before magnetic separation of beads and western blotting of the samples.

2.6.4. Western blotting

Prior to migration, protein samples were supplemented with Laemmli buffer and dithiothreitol 1 M, boiled for 5 min at 95 °C and resolved by SDS-polyacrylamide gel electrophoresis (SDS-PAGE, 12%), along with the ProSieve QuadColor protein marker 4,6 kDa–300 kDa (Lonza). Separated proteins were electrophoretically transferred onto PVDF membranes (GE Healthcare) before protein detection with appropriate primary antibodies and fluorescent dye-coupled secondary antibodies (see Table S4 for details about antibodies). When the proteins could be distinguished by size, a same dye was used for different primary antibodies. Images were acquired using a Typhoon 5 imager (Amersham Biosciences, GE Healthcare).

2.6.5. DNA damage induction

Prior to fixation, HeLa cells were incubated with 25 μM etoposide (Sigma-Aldrich) for 1 h, rinsed with culture medium and maintained for 3 h in culture medium.

2.6.6. Immunofluorescence on HeLa cells

For immunolocalisation, HeLa cells were cultured on 170 μm-thick coverslips (Marienfeld, Lauda-Königshofen, Germany) 24 h before transfection. After etoposide treatment, cells were washed twice with PBS with 500 μM $MgCl_2$ and 500 μM $CaCl_2$ (PBS-S). For whole cell detection, cells were directly fixed with 4% PFA after PBS-S washes. To detect the chromatin-associated fraction and to observe DNA damage foci, cells were permeabilised before fixation as follows: after PBS-S washes, cells were washed once with CSK buffer (10 mM Pipes, pH 7.0, 100 mM NaCl, 300 mM sucrose and 3 mM $MgCl_2$) and incubated 10 min with CSK buffer containing 0.5% Triton X-100, 0.3 mg/ml RNase A (ThermoFisher Scientific) and complete protease inhibitor (Roche). Cells were then washed with PBS-S, fixed with 4% PFA for 20 min and washed with PBS-S. Before staining, cells were blocked with PBS-S/0.1% Tween 20 (PBS-S-T) containing 5% BSA. Cells were incubated with primary antibodies (Table S4) in PBS-S-T/5% BSA and then washed with PBS-S-T and incubated with appropriate fluorescent dye-coupled secondary antibody. After washes in PBS-S-T, coverslips were mounted on glass slides using ProLong® Gold antifade reagent with DAPI (Life Technologies). Imaging was performed using an AX70 epi-fluorescence microscope (Olympus) equipped with a Photometrics CoolSNAP MYO CCD camera. Images were analysed using ImageJ software.

3. Results

The consanguineous family analysed here comprises two sisters affected with POI whose parents are double first cousins (Fig. 1). The proband III-10 had a normal medical history, except for a uterine septum that was removed by surgery at age 20. She presented with infertility, secondary to a severe reduction of ovarian reserve. Married at 18, she had a molar pregnancy at 20 and a subsequent pregnancy ended spontaneously very early. At age 24, oligomenorrhea appeared, and FSH levels rose to 25.36 IU/l at age 25 after one year without hormonal treatment (normal range, 2 to 24 IU/l), with AMH levels at 0.22 ng/ml (normal range 2.2–6.8 ng/ml) and Antral Follicular Count (AFC) = 3. Her husband is healthy, with a normal spermogram. Her sister III-11 presented with secondary amenorrhea. She had normal sexual development during teenage years after normal menarche at 14. Oligomenorrhea developed when she was 16 years old, leading to amenorrhea at age 19, with elevated FSH at 22.7 IU/l rising to 48.8 IU/l, AMH levels below 0.1 ng/ml and AFC = 0. Hormonal replacement therapy induced normal menses, but withdrawal resulted in amenorrhea. Therapeutic trial with high doses of gonadotropins failed to yield follicles. Hormonal dosages at age 30 confirmed the diagnosis of POI (Table 1). Physical examination was normal, with a height of 162 cm and a weight of 83 kg, and the uterus appeared normal on imaging. Her husband is healthy and fertile, with offspring from previous marriages.

WES for the two affected sisters III-10 and III-11, one unaffected sister III-13 and the unaffected mother II-8 generated 51 to 67 million reads per sample with a mean coverage of 67 to 74×. Variant calling identified over 100,000 variants per sample (Tables S1–S2). As it is frequent in consanguineous families, a recessive pathology can emerge because of identity by descent: the children of a consanguineous marriage inherit two copies of an ancestral variant, one through the maternal branch and the other through the paternal branch. Therefore, we filtered variants on the basis of their homozygosity in both patients, heterozygosity in the mother, heterozygosity or absence in the non-affected sister and absence in unrelated fertile in-house controls. Furthermore, we kept variants with a possible impact on the coding sequence and a minor allele frequency (MAF) < 0.01 in databases such as GnomAD. Further filtering on available functional data regarding a possible role in reproduction and fertility yielded only one plausible

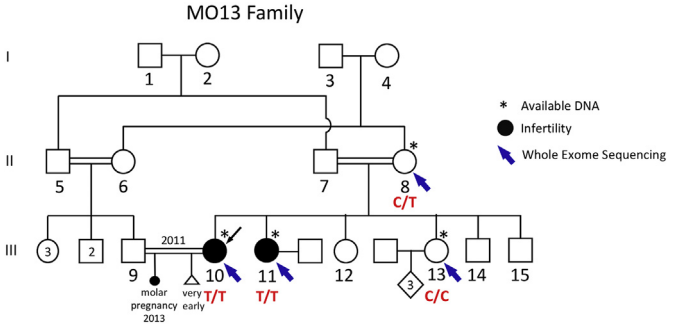

Fig. 1. Identification of a splicing-altering mutation in the coding sequence of MEIOB in a consanguineous POF family. Pedigree of the MO13 family. Double lines indicate consanguineous unions. The black arrow indicates the proband and blue arrows point to the family members that could be analysed by exome sequencing. The genotypes for the mutation in the *MEIOB* gene are indicated below each person, as confirmed by Sanger sequencing (asterisks).

Table 1
Hormonal dosage results for the MO13 patient III-11 at age 30 (May 2017).

Hormones	Dosages in patient	Normal ranges			
		Follicular phase	Ovulatory phase	Luteal phase	Menopause
FSH (IU/l)	48.8	2.9–12	6.3–24	1.5–7	17–95
LH (IU/l)	46.4	1.5–8	9.6–80	0.2–6.5	8–33
Estradiol (nmol/l)	0.149	0.06–0.54	0.16–0.78	0.34–2.1	< 0.2
AMH (ng/ml)	< 0.1	2.2–6.8			
Progesterone (nmol/l)	2.2	0.3–3	2–9	15–60	0.3–3
Testosterone (nmol/l)	0.8	0.4–2			
Prolactin (ng/ml)	6.55	0.7–25			

TSH, free T3 and T4, SHBG, free androgen, androstenedione and DHEA sulfate were within normal ranges.

candidate variant (Table S2). This variant is rs1010446295 in *MEIOB* (annotated as chr16:g.1839255C>T (hg38), NM_001163560.2: c.1218G>A, Fig. 2a), which is predicted to alter splicing of exon 12 with high probability (*i.e.*, p = 0.99 according to AdaBoost and 1 according to Random Forest) [18]. Its MAF in GnomAD database is 0.000018, with only 4 heterozygous individuals and no homozygotes detected in >110,000 genomes. It was absent from the GME Variome dedicated to Middle East populations. Sanger sequencing confirmed that the two affected sisters were indeed homozygous for the *MEIOB* variant, whereas the unaffected family members were either heterozygous or homozygous for the wild-type allele (Fig. S1). *MEIOB* encodes a meiosis-specific factor that binds ssDNA. Our previous expression data in human and mouse show that *MEIOB*/*Meiob* is strongly expressed in the developing ovary during meiosis [9]. Furthermore, its expression profile follows those of typical meiotic genes during ovary development in mice (Fig. S3). We have proposed that MEIOB is a meiotic functional equivalent of RPA1, a mitotic OB domain-containing ssDNA-binding protein [9].

Given the predicted impact of the variant on *MEIOB* pre-mRNA splicing, we considered three potential scenarios according to which the mutation could alter splicing. First, exon 12 bearing the variant could be skipped. Alternatively, the intron downstream of exon 12 could be retained in the mRNA and would be available for translation. Finally, the alteration would induce the removal of both exons 12 and 13 (an exon that can be alternatively spliced out, as in NM_152764) leading to piecing exons 11 and 14 together. In all cases the resulting protein products would be truncated because of frameshifts introducing premature termination codons (PTC). A minigene assay clearly indicated that the mutation induced skipping of exon 12 (Fig. 2b, left panel). This was confirmed *in vivo* by analyzing the illegitimate *MEIOB* transcripts in the leukocytes of proband III-10 (Fig. 2b, middle and right panels, and Fig. S2). Exon 12 skipping disrupts the reading frame, which leads to a frameshift and to the occurrence of a PTC (p.NP_001157032

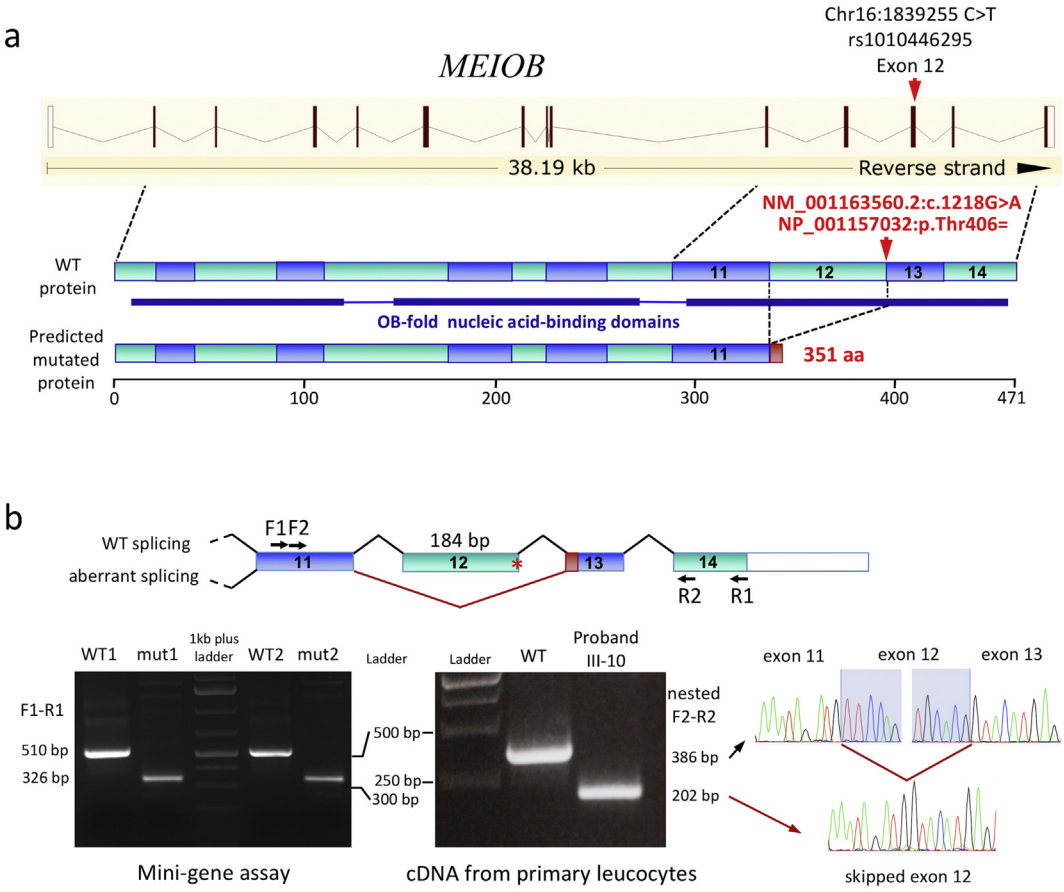

Fig. 2. Exon 12 skipping induced by the *MEIOB* pathogenic variant. a- Representation of the human *MEIOB* gene and its mutated form (from Ensembl, reference transcript NM_001163560.2). The structure of the normal protein is shown below for the longest isoform of 471 amino acids, with coding exons as bars with alternate colours. The mutation (red arrow) lies at the very end of exon 12, which encodes 61 amino acids at the centre of the third OB domain. The second protein structure corresponds to the mutated protein, induced by exon 12 skipping and premature stop codon. The 7-amino acid part of exon 13 read in frameshift is highlighted in red. kb: kilobases. b- Schematic representation of the exon 12 skipping (upper panel) induced by the mutation (red star), along with the detection of aberrant splicing in the *in vitro* minigene assay (bottom panel, left), *in vivo* in the proband's primary leukocytes (bottom panel, center) and the Sanger sequencing of the resulting normal and mutated transcripts. The PCR primers used to amplify the spliced products are located on the exon structure and indicated beside both assays. WT1/mut1 and WT2/mut2 represent 2 independent transfections of the same WT and mutated vectors respectively. WT: wild-type; bp: basepairs, cDNA: complementary DNA.

Cys345Trpfs8). The resulting truncated MEIOB^{mut} protein is expected to contain 351 amino acids, with a normal sequence up to position 344, and would lack most of the third OB-fold and part of its SPATA22-binding domain.

Because the action of MEIOB during meiotic recombination requires its interaction with SPATA22 and the C-terminal part of MEIOB has been shown to mediate such interaction [11,12], we predicted that truncated MEIOB would not interact with SPATA22. To test this, we co-expressed untagged or HA-tagged SPATA22 and the two MYC-FLAG-tagged MEIOB versions in HEK-293 cells that do not express neither MEIOB nor SPATA22 ([11] and https://www.proteomicsdb.org/). As expected, co-immunoprecipitation confirmed the interaction between the full-length MEIOB and SPATA22. By contrast, SPATA22 and truncated MEIOB were barely co-immunoprecipitated, demonstrating that the mutation affected their interaction (Fig. 3).

To test whether the truncation of MEIOB also affected its recruitment to DNA lesions, we mimicked meiotic DSB with etoposide treatment. Etoposide inhibits topoisomerase II, which remains attached to the 5′ extremities of the DSBs it creates. Specifically, we co-expressed HA-tagged SPATA22 and the wild type MYC-FLAG-tagged version of MEIOB (MEIOB^{MF}) or the truncated MYC-FLAG-tagged version of MEIOB (MEIOB$^{MF\text{-}mut}$) in HeLa cells, that do not express neither MEIOB nor SPATA22 (https://www.proteomicsdb.org/). We confirmed by western blot that both versions of MEIOB were indeed expressed (Fig. 4a). After etoposide treatment, the wild-type MEIOB^{MF} and SPATA22 accumulated in the nuclei (Fig. 4b). When MEIOB$^{MF\text{-}mut}$ was expressed with SPATA22, SPATA22 remained diffuse in the entire cell (cytoplasm and nucleus) and MEIOB tended to accumulate in the cytoplasm (Fig. 4b). To focus on proteins recruited to DNA damages, we permeabilised the cells before fixation to retain only the chromatin-associated fraction. The DNA-damage sites were spotted by RPA staining, known to form discrete foci at DSBs. MEIOB^{MF} and SPATA22 colocalised with RPA, confirming their recruitment to etoposide-induced DSBs. Of note, this recruitment to DSBs was detected only when the two proteins were co-expressed (Fig. 4c and d). This confirms the mandatory interaction of the two partners for being recruited at DSBs. In contrast, when the truncated MEIOB$^{MF\text{-}mut}$ was co-expressed with SPATA22, their localization to DSBs was lost (Fig. 4d).

Finally, we estimated the probability of finding other POI cases caused by bi-allelic pathogenic variants in *MEIOB*. For this, we gathered the MAF of all the variants in the coding region of *MEIOB* referenced in GnomAD (as of February 2019). We focused on those variants predicted to be pathogenic or possibly damaging by at least 6 out of 11 predictors of functional impact. The cumulative MAF of the 149 predicted pathogenic variants was 0.01349. This corresponds to one woman out of about 11,000 (*i.e.*, $2/0.01349^2$), who would be either homozygous or compound heterozygous for *MEIOB* damaging variants.

4. Discussion

Our genetic analysis allowed us to identify a variant in the *MEIOB* gene responsible for POI in a consanguineous family. Our study of the impact of the mutation on *MEIOB* pre-mRNA splicing *in vitro* and *in vivo* showed that exon 12 was skipped. In principle, we cannot exclude a nonsense-mediated decay (NMD) of the mutated transcripts, because the PTC does not lie in the last exon. However, NMD is not certain because of the small size of exon 13 (87 bases). In such conditions, the ribosome might still be able to remove the Exon Junction Complex at the boundary between exons 13 and 14 when reaching the PTC (thus abrogating NMD). The fact that the wild-type and mutated cDNAs from the patient's leukocytes yielded PCR bands of similar intensities when amplified in similar conditions from similar amounts of cDNA indeed argues against NMD of the mutated transcript. However, even in

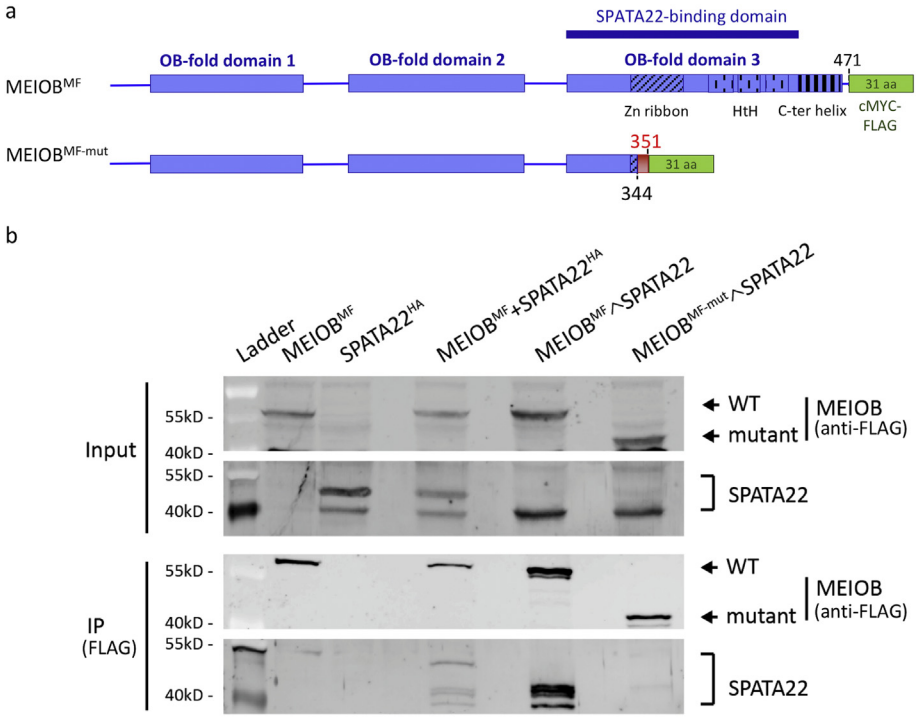

Fig. 3. The MEIOB-truncating mutation disrupts MEIOB-SPATA22 interaction. a- Schematic representation of MEIOB constructs. The wild-type MEIOB^{MF} contains 3 OB-fold domains and a C-terminal cMyc-FLAG tag (in green). The third OB-fold domain contains an additional Zinc ribbon domain and a helix-turn-helix (HtH), encoded by the end of exon 11 and exons 12, 13, and part of exon 14, and corresponds to the SPATA22-binding domain [11,12]. The truncated MEIOB$^{MF\text{-}mut}$ contains the wild-type sequence up to position 344 encompassing only the beginning of the zinc ribbon domain plus seven residues read in frameshift (in red) before the cMyc-FLAG tag. b- SPATA22 co-immunoprecipitation with MEIOB is lost in *MEIOB* mutant. MEIOB^{MF} or MEIOB$^{MF\text{-}mut}$, HA-tagged SPATA22 (SPATA22^{HA}), or untagged SPATA22 (SPATA22) were expressed in HEK-293 cells. MEIOB^{MF}^SPATA22 indicates that MEIOB^{MF} and SPATA22 were expressed from a single plasmid. MEIOB is immunoprecipitated with an anti-FLAG antibody (IP-FLAG). MEIOB is revealed with an anti-FLAG antibody and SPATA22 with an anti-SPATA22 antibody. The ProSieve QuadColor protein marker 4,6 kDa–300 kDa (Lonza) was run on the left (Ladder).

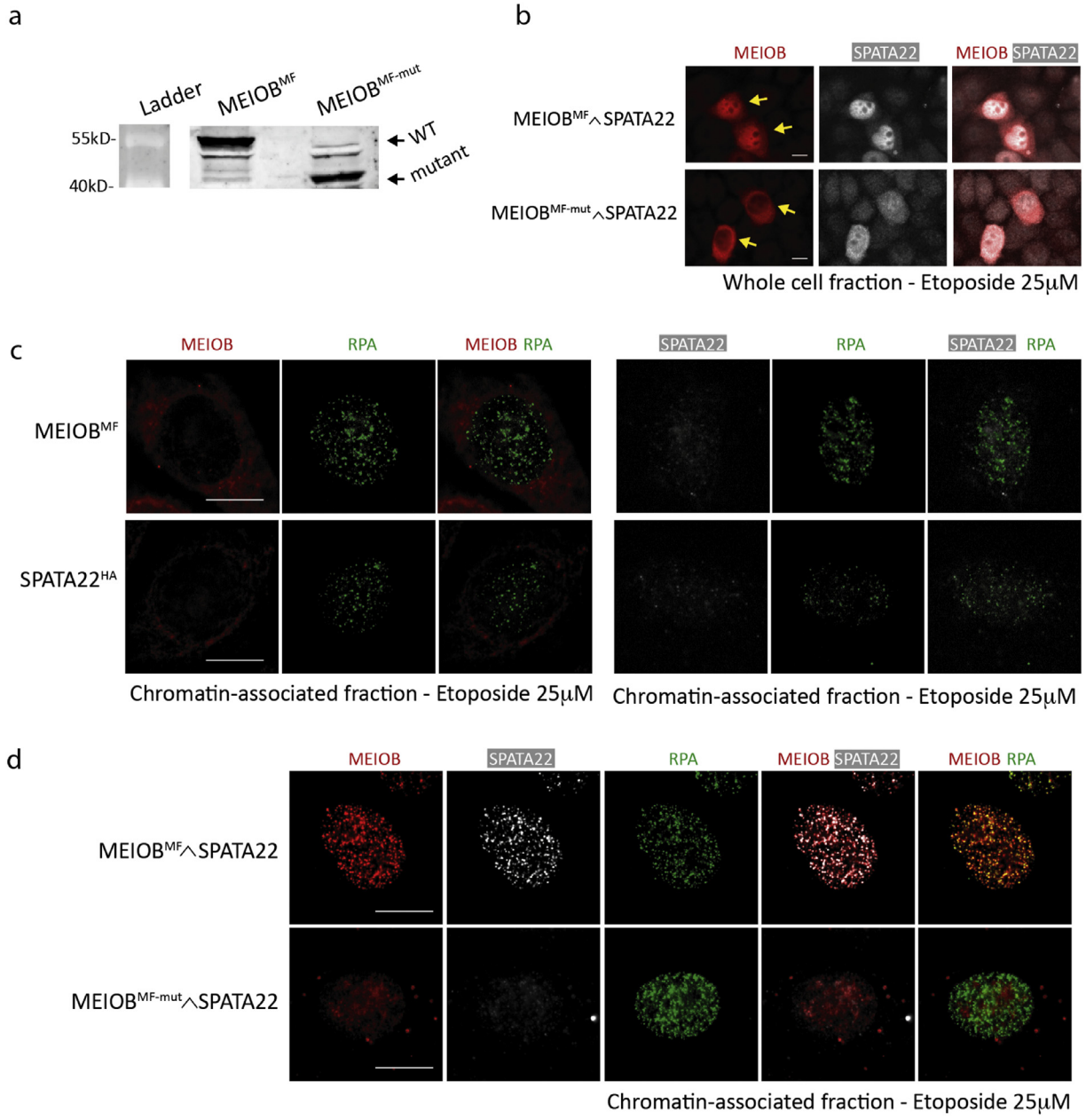

Fig. 4. The MEIOB-truncating mutation disrupts MEIOB-SPATA22 recruitment to DNA damage foci. a-b- The truncated form of MEIOB is stable when expressed in HeLa cells. a- Western blot showing the expression of the wild-type ($MEIOB^{MF}$) and the truncated forms ($MEIOB^{MF-mut}$) of MEIOB transfected in HeLa cells. The ProSieve QuadColor protein marker 4,6 kDa–300 kDa (Lonza) was run on the left (Ladder). b- $MEIOB^{MF}$ or $MEIOB^{MF-mut}$ and SPATA22 were co-expressed from a single plasmid MEIOB∧SPATA22 in HeLa cells before exposure to etoposide (25 μM). Cells were fixed in PFA without pre-permeabilisation to retain both cytoplasmic and nuclear fractions. Antibodies were used to immunostain MEIOB (red) and SPATA22 (white). Yellow arrows highlight transfected cells expressing both MEIOB and SPATA22. c-d- The truncation prevents MEIOB recruitment with SPATA22 to DSBs. $MEIOB^{MF}$ or $MEIOB^{MF-mut}$ and $SPATA22^{HA}$ were expressed in HeLa cells before exposure to etoposide. Cells were permeabilised before fixation in PFA to analyse the chromatin-associated fraction of proteins. RPA foci are formed at DNA damage sites. c- MEIOB or SPATA22 alone are not recruited to DNA damage sites. d- When co-expressed, $MEIOB^{MF}$ and SPATA22 are recruited to DNA-damage sites and colocalise with RPA. This colocalisation is not observed for the truncated $MEIOB^{MF-mut}$. Antibodies are used to immunostain MEIOB (red), SPATA22 (white), and RPA (green). Scale bar = 10 μm in all panels.

the presence of NMD, the conclusion pointing to the causality of the variant would hold.

Recent studies identified the C-terminal part of MEIOB between positions 294 and 450 as the SPATA22-binding domain of the protein, which is required for the interaction between the two proteins and for their recruitment to DSBs [11,12]. In the present study, we show that the truncation induced by the mutation strongly affects this interaction and prevents the recruitment of both MEIOB and SPATA22 to DSBs.

Meiob knock-out mice are infertile and unable to complete meiotic recombination, as shown by the persistence of unrepaired DNA breaks. Indeed, the mutated ovaries are completely devoid of oocytes by early postnatal days [9,10]. The results described here are consistent with the phenotype observed in $Meiob^{-/-}$ female mice and highlight the importance of the MEIOB-SPATA22 interaction *in vivo*. Recently, a homozygous missense (N64I) was reported in a consanguineous Israeli Arab family with 4 azoospermic brothers [20]. This missense substitution concerned a highly conserved residue within a DNA binding domain of the protein. Although this variant is likely to be causal, it is always difficult to provide such a proof for a missense mutation, especially when the status of unaffected family members cannot be assessed and/or in the absence of a knock-in model. Causality is more obvious for a truncating mutation, as the one described here or as the homozygous

frameshift mutation very recently reported in two azoospermic brothers from a consanguineous family and an unrelated azoospermic patient [21]. This mutation is predicted to induce the truncation of the C-terminal part of MEIOB, and the complete impairment of spermatocyte maturation in these patients.

Our study increases the number of genes whose products are involved in meiotic recombination as a cause of female infertility [4–7,22,23]. It also provides the first example of a pathogenic variant in a gene encoding a SSB protein involved in POI. Although we report only one family with two POI cases, we think that we provide the level of evidence required to formally implicate MEIOB in POI. We expect pathogenic variants in MEIOB to be a rare cause of POI, as reported for all known 'POI' genes for obvious Darwinian reasons. Based on available data, we estimated the cumulative frequency of all known MEIOB variants predicted to be pathogenic. This analysis yielded an estimate of 1 woman out of 11,000 who would be either homozygous or compound heterozygous for MEIOB clearly damaging variants. We hope that the publication of the first pathogenic variant in *MEIOB* will trigger interest in this gene. Finding novel supporting cases will help improve the diagnosis and counselling of patients with POI. Finally, we hypothesise that mutations in other SSB proteins could explain other cases of ovarian insufficiency, be it syndromic (when the protein is not meiosis-specific) or isolated.

Acknowledgements

SC and RAV express their sincere thanks to the family for their participation in this research. We acknowledge the CIGEX (CEA, Fontenay aux Roses, France) for plasmid construction and J. Ribeiro for the initial characterization of MEIOB-SPATA22 interaction.

Funding sources

This study was supported by Université Paris Diderot (SC, BL, ALT, RAV, GL), the Fondation pour la Recherche Médicale (Labelisation Equipes DEQ20150331757, SC, BL, ALT, RAV), the Fondation ARC pour la recherche contre le cancer (CP, EM, GL), the Commissariat à l'Energie Atomique (CP, EM), and the Institut Universitaire de France (GL). The funders had no role in study design, data collection, data analysis, interpretation or writing of the report.

Declaration of interests

The authors declare no conflict of interest.

Data sharing

Non-identifying data supporting the claims made in this paper are available upon request after its publication. Requests should be addressed to the corresponding authors of this paper: Profs. R. A. Veitia (reiner.veitia@ijm.fr) or to J.S. Yunis (jsy@netvision.net.il).

Author contributions

RAV, JSY and SS conceived and headed the project. JSY performed the patient recruitment and phenotyping. SC performed the WES data analysis and variant interpretation. BL and ALT set up and performed the *in vitro* functional assay. BL performed the genomic DNA sequencing. NDF performed the patient's illegitimate MEIOB mRNA splicing analysis. CP, EM and GL set up and performed the functional assays in cells. SC and RAV drafted the manuscript with input from all authors. All authors approved the final version of the manuscript.

Appendix A. Supplementary data

Supplementary data to this article can be found online at https://doi.org/10.1016/j.ebiom.2019.03.075.

References

[1] Rossetti R, Ferrari I, Bonomi M, Persani L. Genetics of primary ovarian insufficiency. Clin Genet 2017;91:183–98. https://doi.org/10.1111/cge.12921.
[2] Persani L, Rossetti R, Cacciatore C. Genes involved in human premature ovarian failure. J Mol Endocrinol 2010;45:257–79. https://doi.org/10.1677/JME-10-0070.
[3] Huhtaniemi I, Hovatta O, La Marca A, Livera G, Monniaux D, Persani L, et al. Advances in the molecular pathophysiology, genetics, and treatment of primary ovarian insufficiency. Trends Endocrinol Metab 2018;29:400–19. https://doi.org/10.1016/j.tem.2018.03.010.
[4] Caburet S, Arboleda VA, Llano E, Overbeek PA, Barbero JL, Oka K, et al. Mutant cohesin in premature ovarian failure. N Engl J Med 2014;370:943–9. https://doi.org/10.1056/NEJMoa1309635.
[5] AlAsiri S, Basit S, Wood-Trageser MA, Yatsenko SA, Jeffries EP, Surti U, et al. Exome sequencing reveals MCM8 mutation underlies ovarian failure and chromosomal instability. J Clin Invest 2015;125:258–62. https://doi.org/10.1172/JCI78473.
[6] Wood-Trageser MA, Gurbuz F, Yatsenko SA, Jeffries EP, Kotan LD, Surti U, et al. MCM9 mutations are associated with ovarian failure, short stature, and chromosomal instability. Am J Hum Genet 2014;95:754–62. https://doi.org/10.1016/j.ajhg.2014.11.002.
[7] Wang J, Zhang W, Jiang H, Wu B-L. Primary ovarian insufficiency collaboration. Mutations in HFM1 in recessive primary ovarian insufficiency. N Engl J Med 2014;370:972–4. https://doi.org/10.1056/NEJMc1310150.
[8] de Vries L, Behar DM, Smirin-Yosef P, Lagovsky I, Tzur S, Basel-Vanagaite L. Exome sequencing reveals SYCE1 mutation associated with autosomal recessive primary ovarian insufficiency. J Clin Endocrinol Metab 2014;99:E2129–32. https://doi.org/10.1210/jc.2014-1268.
[9] Souquet B, Abby E, Hervé R, Finsterbusch F, Tourpin S, Le Bouffant R, et al. MEIOB targets single-strand DNA and is necessary for meiotic recombination. PLoS Genet 2013;9:-e1003784. https://doi.org/10.1371/journal.pgen.1003784.
[10] Luo M, Yang F, Leu NA, Landaiche J, Handel MA, Benavente R, et al. MEIOB exhibits single-stranded DNA-binding and exonuclease activities and is essential for meiotic recombination. Nat Commun 2013;4:2788. https://doi.org/10.1038/ncomms3788.
[11] Xu Y, Greenberg RA, Schonbrunn E, Wang PJ. Meiosis-specific proteins MEIOB and SPATA22 cooperatively associate with the single-stranded DNA-binding replication protein a complex and DNA double-strand breaks. Biol Reprod 2017;96:1096–104. https://doi.org/10.1093/biolre/iox040.
[12] Ribeiro J, Dupaigne P, Duquenne C, Veaute X, Petrillo C, Saintome C, et al. MEIOB and SPATA22 resemble RPA subunits and interact with the RPA complex to promote meiotic recombination. BioRxiv 2018:358242. https://doi.org/10.1101/358242.
[13] Gnirke A, Melnikov A, Maguire J, Rogov P, LeProust EM, Brockman W, et al. Solution hybrid selection with ultra-long oligonucleotides for massively parallel targeted sequencing. Nat Biotechnol 2009;27:182–9. https://doi.org/10.1038/nbt.1523.
[14] Liu X, Jian X, Boerwinkle E. dbNSFP: a lightweight database of human nonsynonymous SNPs and their functional predictions. Hum Mutat 2011;32:894–9. https://doi.org/10.1002/humu.21517.
[15] Liu X, Jian X, Boerwinkle E. dbNSFP v2.0: a database of human non-synonymous SNVs and their functional predictions and annotations. Hum Mutat 2013;34:E2393–402. https://doi.org/10.1002/humu.22376.
[16] Liu X, Wu C, Li C, Boerwinkle E. dbNSFP v3.0: a one-stop database of functional predictions and annotations for human nonsynonymous and splice-site SNVs. Hum Mutat 2016;37:235–41. https://doi.org/10.1002/humu.22932.
[17] Jagadeesh KA, Wenger AM, Berger MJ, Guturu H, Stenson PD, Cooper DN, et al. M-CAP eliminates a majority of variants of uncertain significance in clinical exomes at high sensitivity. Nat Genet 2016;48:1581–6. https://doi.org/10.1038/ng.3703.
[18] Jian X, Boerwinkle E, Liu X. In silico prediction of splice-altering single nucleotide variants in the human genome. Nucleic Acids Res 2014;42:13534–44. https://doi.org/10.1093/nar/gku1206.
[19] Sambrook J, Russell DW. Molecular Cloning: A Laboratory Manual. . 3Cold Spring Harbor, N.Y: Cold Spring Harbor Laboratory Press; 2001.
[20] Gershoni M, Hauser R, Yogev L, Lehavi O, Azem F, Yavetz H, et al. A familial study of azoospermic men identifies three novel causative mutations in three new human azoospermia genes. Genet Med Off J Am Coll Med Genet 2017;19:998–1006. https://doi.org/10.1038/gim.2016.225.
[21] Gershoni M, Hauser R, Barda S, Lehavi O, Arama E, Pietrokovski S, et al. A new MEIOB mutation is a recurrent cause for azoospermia and testicular meiotic arrest. Hum Reprod 2019. https://doi.org/10.1093/humrep/dez016.
[22] Qin Y, Guo T, Li G, Tang T-S, Zhao S, Jiao X, et al. CSB-PGBD3 mutations cause premature ovarian failure. PLoS Genet 2015;11. https://doi.org/10.1371/journal.pgen.1005419 e1005419.
[23] Zangen D, Kaufman Y, Zeligson S, Perlberg S, Fridman H, Kanaan M, et al. XX ovarian dysgenesis is caused by a PSMC3IP/HOP2 mutation that abolishes coactivation of estrogen-driven transcription. Am J Hum Genet 2011;89:572–9. https://doi.org/10.1016/j.ajhg.2011.09.006.